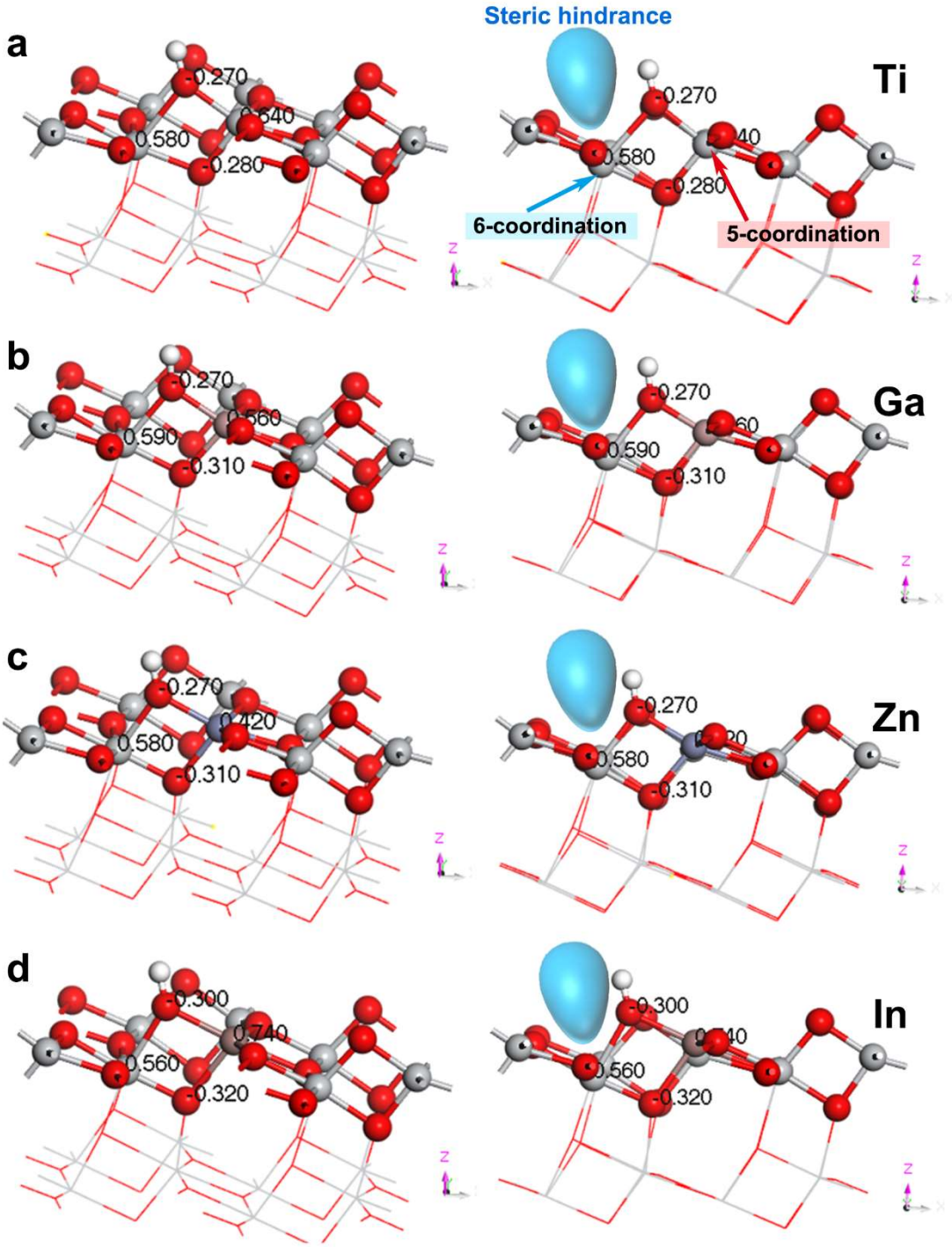

Fig. S1 Models of hydrogenated TiO_2 with Ti_{5c} replaced by different metal dopants. **a,** Ti, **b,** Ga, **c,** Zn, **d,** In. The higher steric hindrance is marked in blue. The color of Ti, O and H atoms are grey, red and white, respectively.

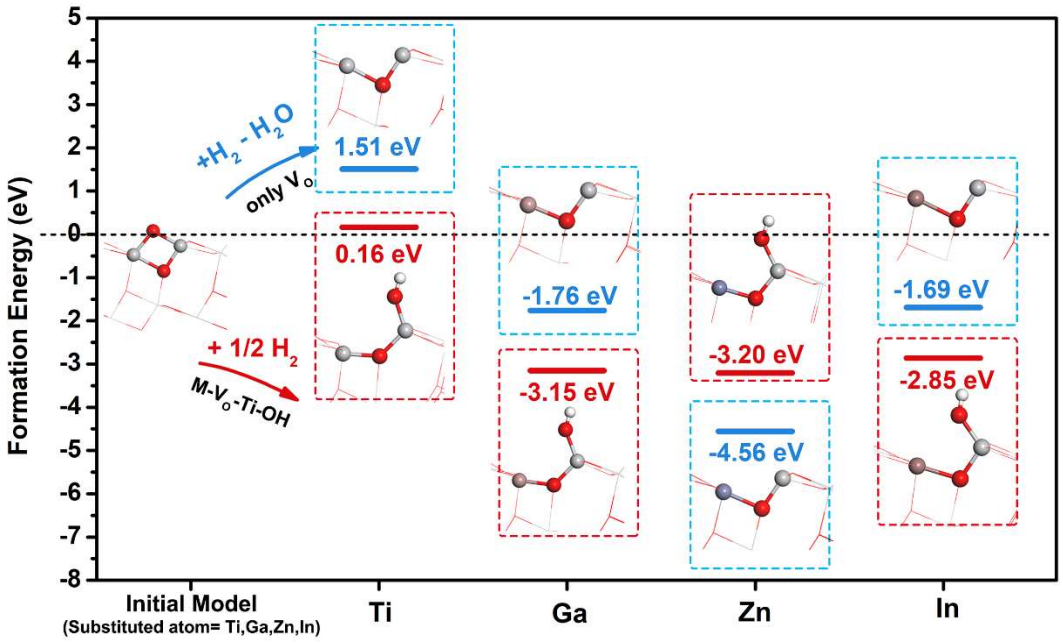

Fig. S2 Formation energies of M-V_O-Ti only with Vo and M-V_O-Ti-OH with both Vo and Ti-OH.

$$E(M\text{-}V_O\text{-}Ti) = E_{final} - E_{initial} - E_{H2} + E_{H2O}$$

$$E(M\text{-}V_O\text{-}Ti\text{-}OH) = E_{final} - E_{initial} - 1/2\ E_{H2}$$

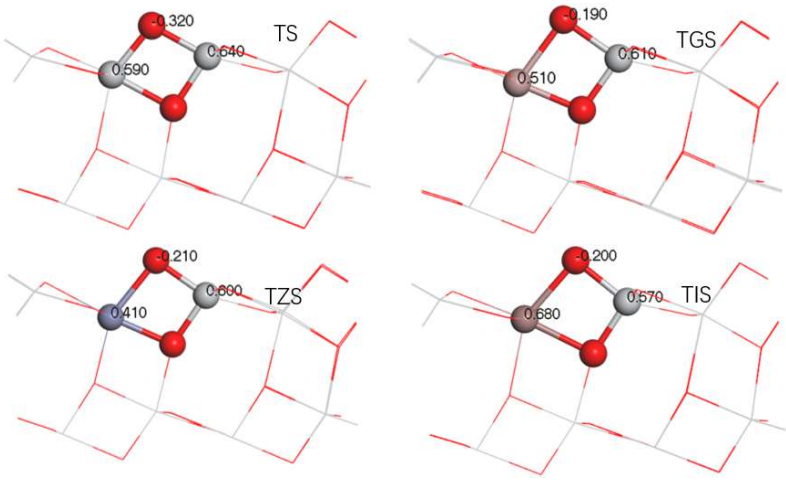

Fig. S3 Configuration models of Metal-doped TiO_2 by replacing Ti_{6c} with different metal dopants (Ga, Zn, In). TS is the non-dope TiO_2. TGS, TZS and TIS are structures with Ga, Zn and In, respectively. The Hirshfeld charge is shown in black font.

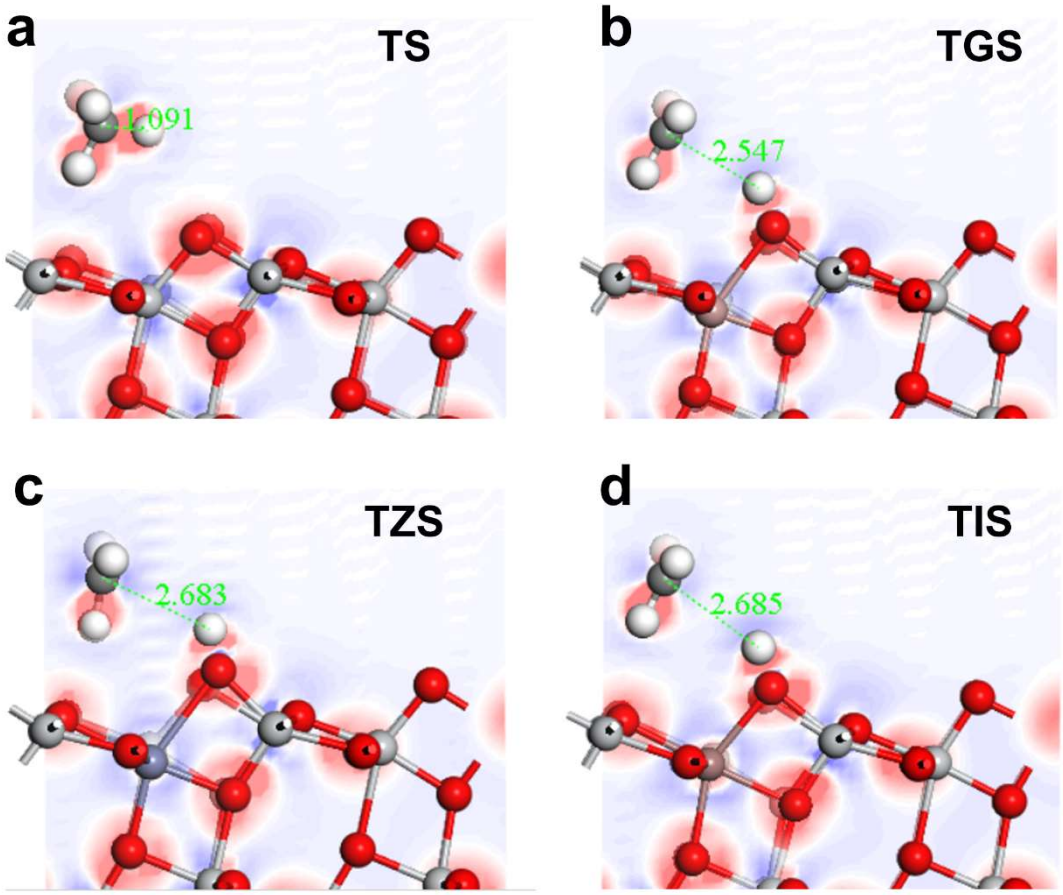

Fig. S4 C-H cleavage over models of **a,** TS, **b,** TGS, **c,** TZS, **d,** TIS.

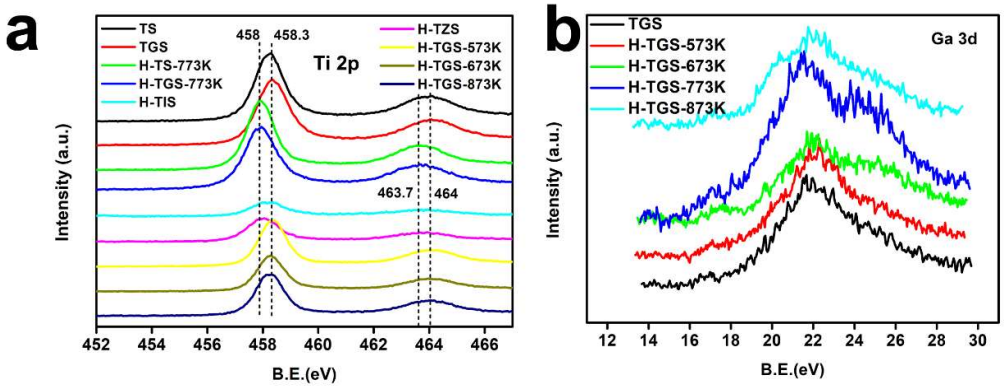

Fig. S5 **a,** Ti 2p, **b,** Ga 3d XPS patterns of different samples.

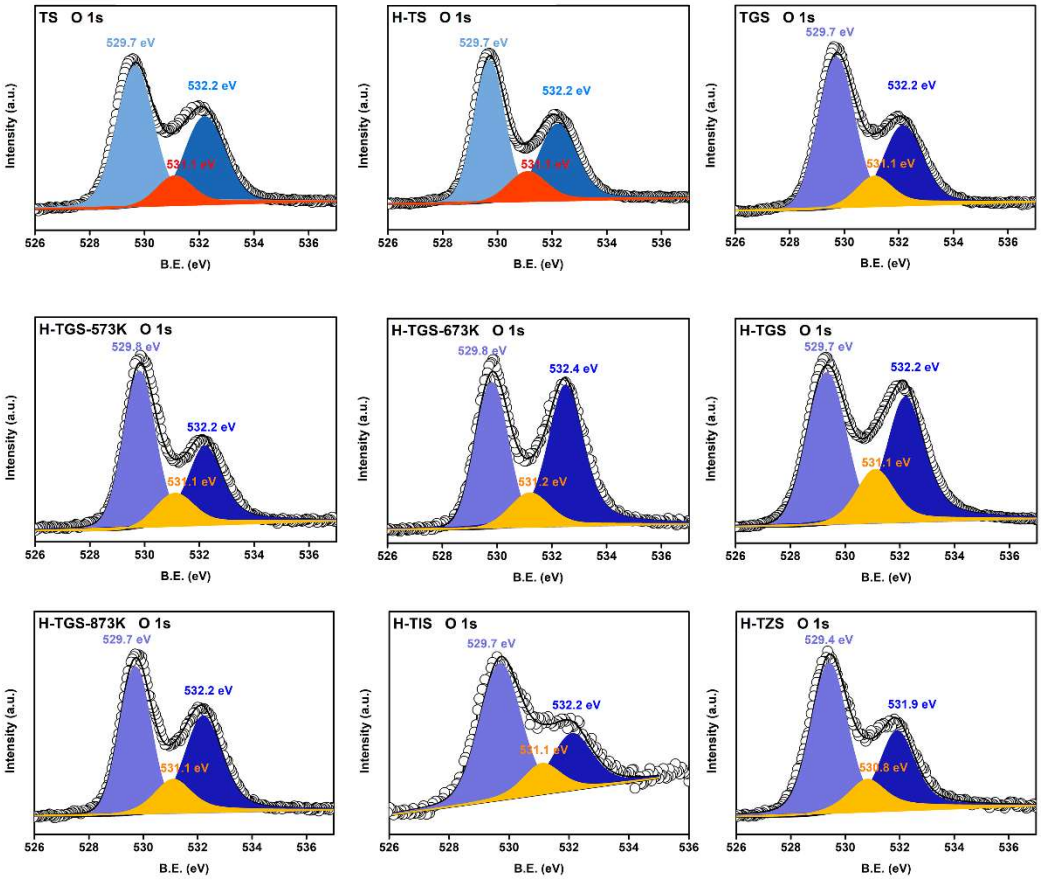

Fig. S6 O 1s XPS patterns of different samples.

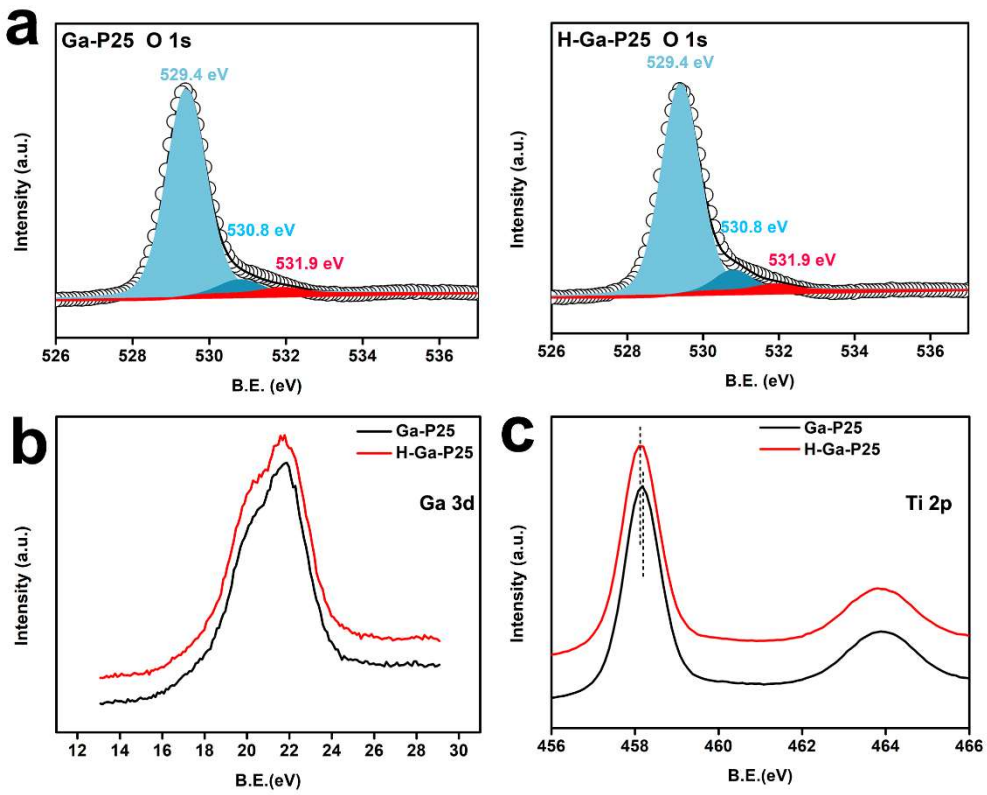

Fig. S7 **a,** O 1s, **b,** Ga 3d and **c,** Ti 2p XPS patterns of Ga-P25 and H-Ga-P25.

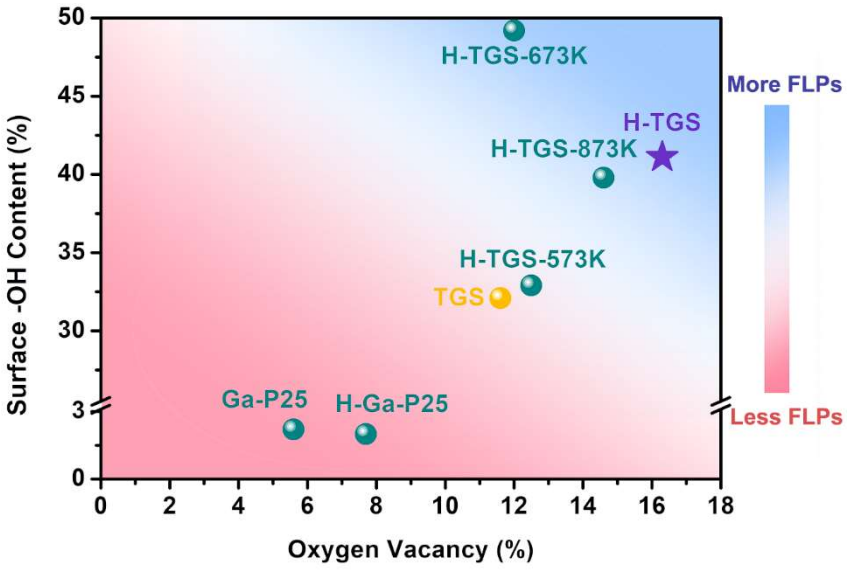

Fig. S8 Concentrations of surface -OH and Vo of different samples.

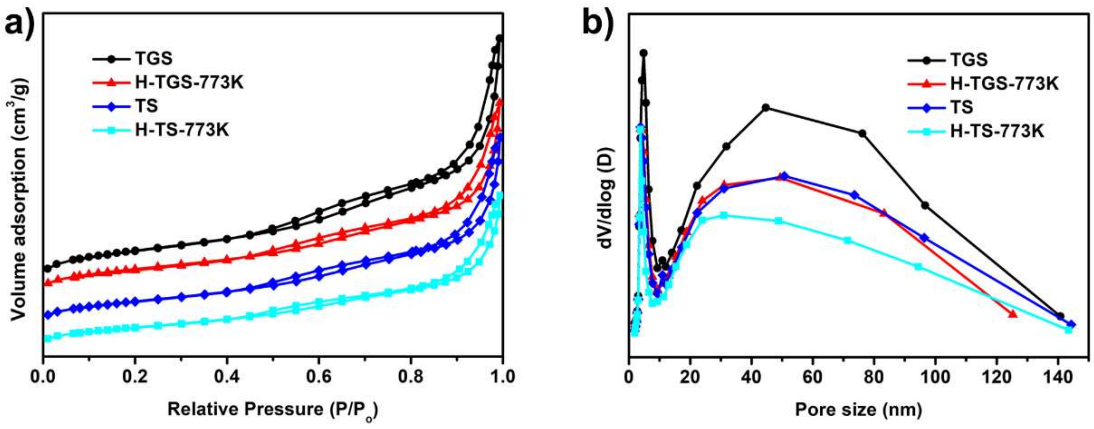

Fig. S9 **a,** N_2 adsorption-desorption isotherm and **b,** pore size distribution of different samples.

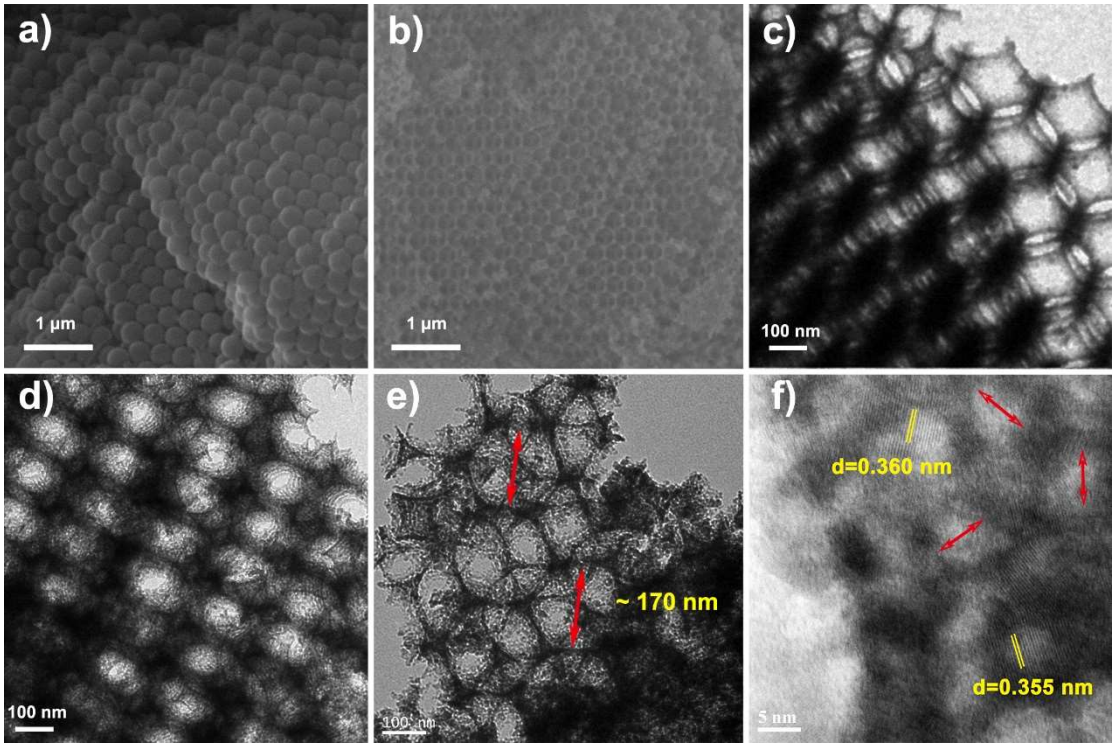

Fig. S10 **a,** SEM image of polystyrene microspheres (PS), **b, c,** SEM and TEM images of TGS, **d,** TEM image of TS, **e,** TEM image of H-TGS **f,** HRTEM image of H-TGS. The red double arrow indicates the porous structure.

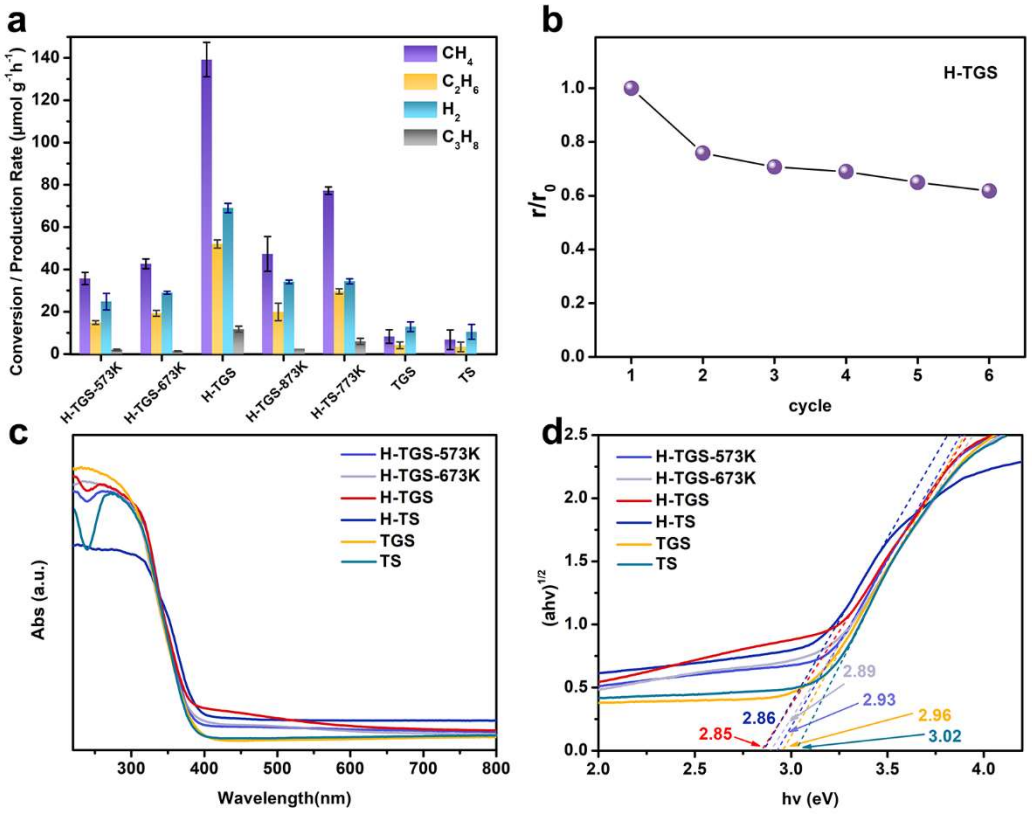

Fig. S11 **a,** Conversion and production rates for photocatalytic NOCM. **b**, Stability of H-TGS after cycling 6 times. **c**, UV−vis diffuse reflectance spectra and **d**, band gaps of different samples.

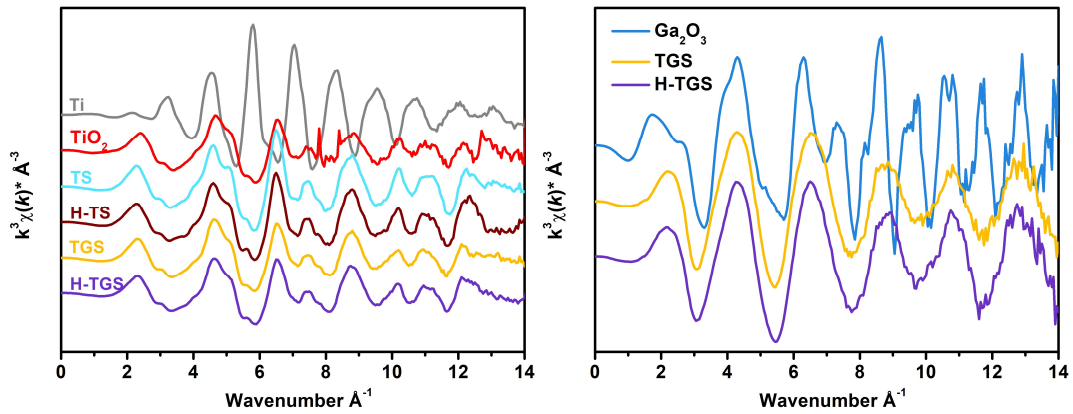

Fig. S12 Ti and Ga K-edge extended X-ray absorption fine structure (EXAFS) spectra.

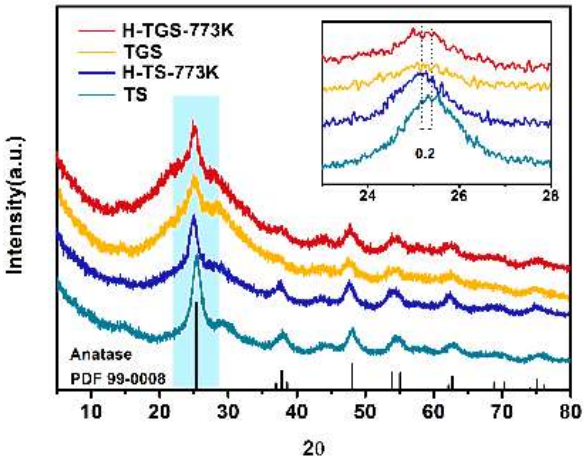

Fig. S13 XRD patterns of different samples, built-in is the enlarged range of 23-28 °.

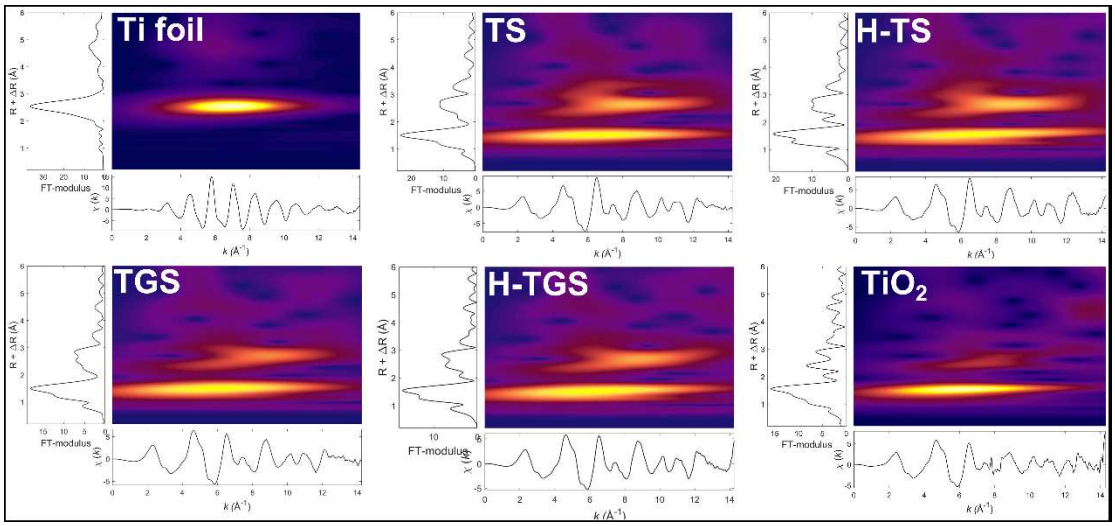

Fig. S14 WT-EXAFS signals of Ti foil, TS, H-TS, TGS, H-TGS and TiO_2.

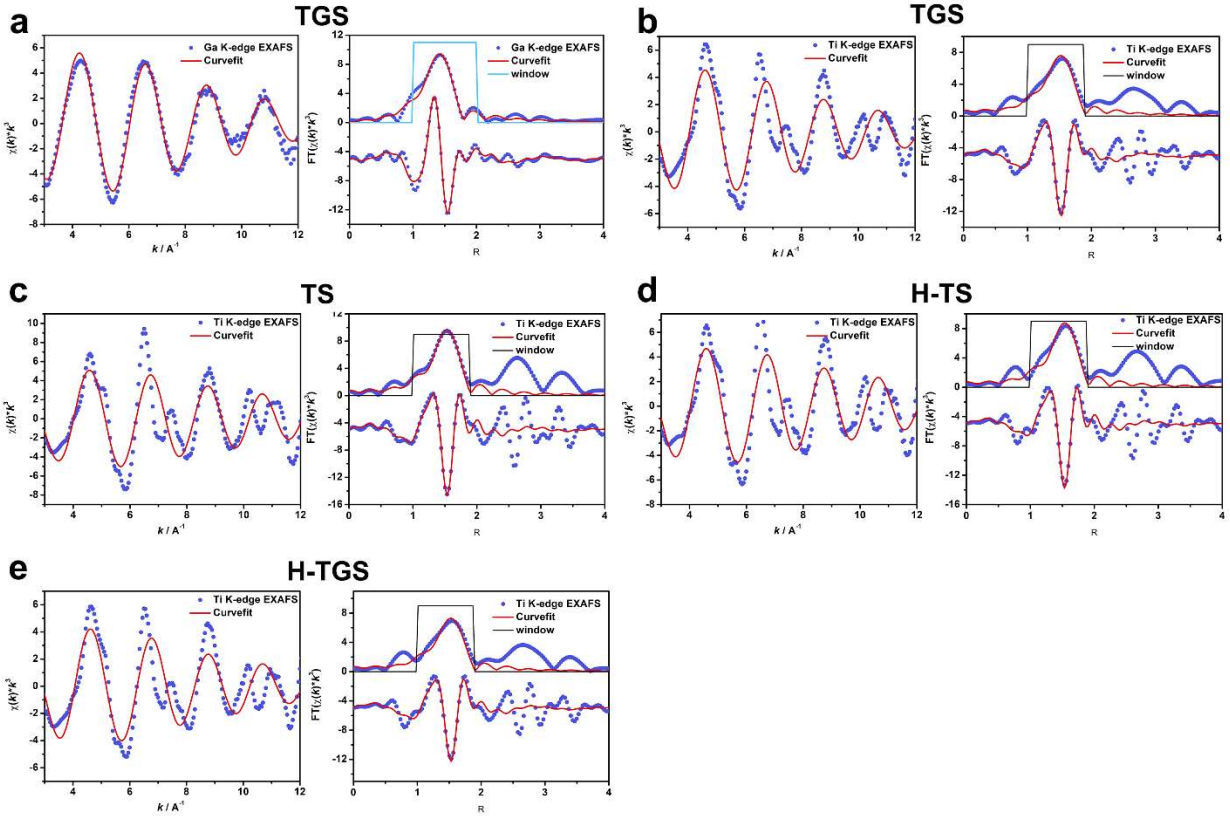

Fig. S15 Ga or Ti K-edge EXAFS (points) and the curvefit (line) for different samples, shown in k^3-weighted k-space (left) or in R-space (right). The data are k^3-weighted and not phase-corrected.

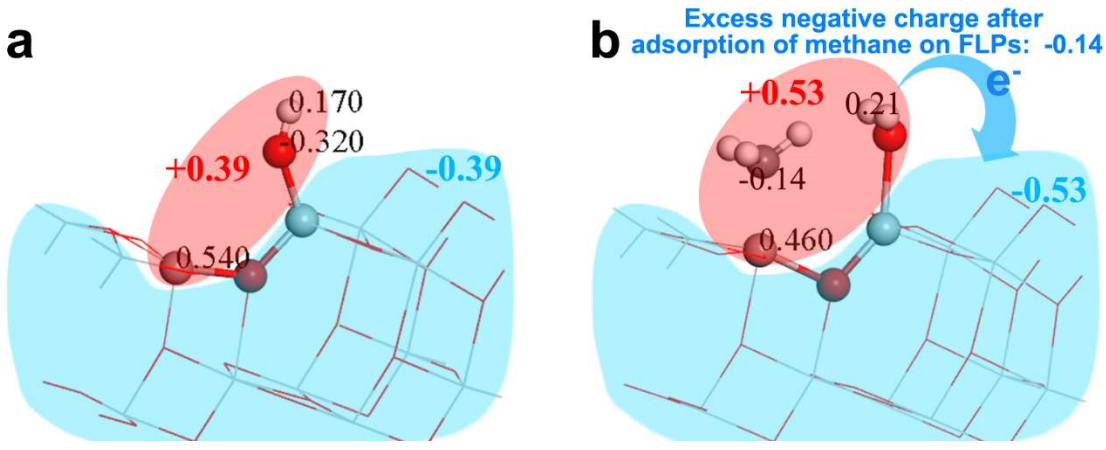

Fig. S16 The excess negative charge from -CH_3 and -H adsorption.

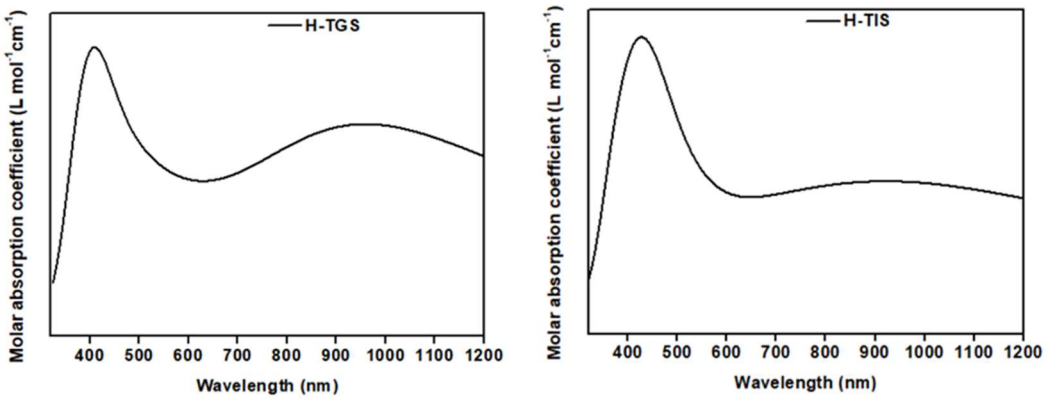

Fig. S17 The calculated absorption band is mainly composed of electronic transition in the range of 400-550 nm. Excited state: H-TGS, 2.4683 eV, f = 0.04260; H-TIS, 2.6038 eV, f = 0.02020.

Table S1. The formation energies for different hydrogenated and metal-doped structures.

	E(6c-substitute)	E(5c-substitute)	E(V_O)	E-adsorb CH_4	ΔE
Ga	-3.15	-3.29	-1.76	1.08	0.13
In	-2.85	-3.23	-1.69	0.34	0.36
Ti	0.16	0.01	1.51	1.26	0.15
Zn	-3.20	-3.30	-4.56	-0.13	0.09

ΔE represents the energy difference between six-coordinated substitution and five coordinate substitution.

$$E(V_O) = E_{final} - E_{initial} - E_{H2} + E_{H2O}$$

$$E(6c\text{-substitute}) \text{ or } E(5c\text{-substitute}) = E_{final} - E_{initial} - 1/2\ E_{H2}$$

Table S2. Fine deconvolution of the O 1s XPS spectra

Catalyst	Oxygen vacancy (%)	Surface -OH (%)
H-TGS-573K	12.5	32.9
H-TGS-673K	12.0	49.2
H-TGS	16.3	41.1
H-TGS-873K	14.6	39.8
TGS	11.6	32.1
H-TS	12.9	35.3
TS	10.4	34.1
H-TIS	14.2	26.8
H-TZS	13.5	30.5
Ga-P25	5.6	2.2
H-Ga-P25	7.7	2.0

Table S3. Activities of various samples for photocatalytic NOCM

Photocatalyst	Average yield (μmol g^{-1} h^{-1})			Conversion rate of CH_4 (μmol g^{-1} h^{-1})	error bar of Conversion rate of CH_4	Selectivity of C_2H_6 (%)
	C_2H_6	C_3H_8	H_2			
H-TGS-573K	14.88	2.00	24.75	35.75	2.83	88
H-TGS-673K	19.25	1.38	29	42.63	2.30	93
H-TGS	52.00	11.75	69.06	139.25	8.13	82
H-TGS-873K	19.91	2.50	34.13	47.33	8.24	89/
H-TS	29.63	6.00	34.38	77.25	1.77	83
TGS	4.13	/	12.88	8.25	3.18	/
TS	3.38	/	10.50	6.75	4.60	/
H-TIS	37.38	1.63	28.25	79.63	2.65	96/
H-TZS	14.75	/	21.88	29.50	2.83	/
H-TGS Pyridine	7.17	/	9.92	14.33	3.30	/
H-TGS Pyrrole	5.42	/	7.50	10.83	0.71	/
H-P25	7.63	/	12.50	15.25	1.77	/
H-Ga-P25	8.38	/	1.8	16.75	1.06	/
Ga-P25	1.13	/	0.88	2.25	1.06	/

Reaction conditions were as follows: samples, 2 mg; reaction time, 4 h; reactant, 44.6 μmol of methane; light source, 300 W Xe lamp; reaction temperature, room temperature; quartz reactor, 44 cm^3. The products were analyzed by gas chromatography with flame-ionization and thermal conductivity detector.

Table S4. Contents of LA and BA detected by Pyridine-IR spectra

	Desorb at 473 K	
	BA (mmol/g)	LA (mmol/g)
TS	0.00000	0.02958
TGS	0.00000	0.05448
H-TS	0.00238	0.04548
H-TGS	0.00540	0.05550

Table S5. Curvefit parameters of Ti K-edge[a] EXAFS for the shell of first-nearest neighbors in TGS, H-TGS, TS and H-TS.

Path	Coordination number	ΔR/ Å	Radial distance/ Å	σ^2/ Å^2	ΔE	R-Factor
TGS	Ti-O 4.7(±1.1)	-0.03	1.95(±0.02)	0.006(±0.003)	-0.8(±3.2)	0.012
H-TGS	Ti-O 4.2(±0.9)	-0.02	1.95(±0.02)	0.006(±0.003)	-0.3(±3.1)	0.013
TS	Ti-O 4.9(±0.9)	-0.05	1.95(±0.02)	0.004(±0.002)	-2.3(±2.7)	0.009
H-TS	Ti-O 4.5(±1.0)	0.02	1.96(±0.02)	0.004(±0.003)	-1.0(±3.3)	0.017

[a]S_0^2 was fixed as 0.80 for Ti K-edge EXAFS. Data ranges; $3.0 \le k \le 12.3$ Å-1, $1.0 \le R \le 1.9$ Å. The number of variable parameters is 4, out of a total of 5.1 independent data points.

Table S6. Curvefit parameters of Ga K-edge[b] EXAFS for the shell of first-nearest neighbors in TGS, H-TGS,

Path	Coordination number	ΔR/ Å	Radial distance/ Å	σ^2/ Å^2	ΔE	R-Factor
TGS	Ga-O 5.0(±0.5)	-0.03	1.85(±0.01)	0.006(±0.001)	-1.2(±1.5)	0.005
H-TGS	Ga-O 4.7(±0.5)	-0.02	1.85(±0.01)	0.005(±0.001)	-0.2(±1.7)	0.007

[b]S_0^2 was fixed as 0.85 for Ga K-edge EXAFS. Data ranges; $3.0 \le k \le 12.0$ Å-1, $1.0 \le R \le 2.0$ Å. The number of variable parameters is 4, out of a total of 5.6 independent data points.